Computers & Industrial Engineering 137 (2019) 106081

Contents lists available at ScienceDirect

Computers & Industrial Engineering

journal homepage: www.elsevier.com/locate/caie

Optimal design of an attribute control chart for monitoring the mean of autocorrelated processes

Wenhui Zhou, Cheng Cheng, Zhibin Zheng*

School of Business Administration, South China University of Technology, Guangzhou 510000, Guangdong, China

ARTICLE INFO

Keywords:
Attribute chart
Autocorrelated processes
Mean shifts
First order autoregressive process
Attribute inspection

ABSTRACT

Several control charts have been proposed to employ attribute inspection to monitor the process mean. However, these control charts are not applicable in many industrial applications where the process variables are highly autocorrelated due to the assumption that the sequence of process observations is statistically independent. Motivated by the simple implementation and good performance of these charts, in this paper, an attribute chart is proposed to monitor the mean of the autocorrelated processes by assuming the distribution of observations follows the First Order Autoregressive ($AR(1)$) process. To optimally design the proposed chart, a more tractable approach is introduced to compute average run length (ARL) by adopting the Stein-Chen method. In addition, a comparison of the proposed control chart with np_x chart is presented to investigate the performance of the proposed chart and the effect of autocorrelation. A sensitivity analysis is also provided to study the robustness of the proposed chart. Finally, an industry example is given to illustrate how to apply proposed chart to the manufacturing process.

1. Introduction

Statistical process control (SPC) methods are widely employed to monitor the manufacturing process and improve quality. As one of the major tools, various statistical control charts have been developed to monitor the process variation. Particularly, the attribute control charts, such as p, np, c and *CRL* charts, are widely recognized in practice and also extensively investigated and improved by many researchers owing to their simplicity in implementation.

Although Montgomery (2007) pointed out that attribute inspection is significantly less expensive and time-consuming on a per-unit basis than variable-type inspection, attribute charts are commonly believed to be inefficient to deal with a quality characteristic that is of a variable type. Motivated by this, Wu and Jiao (2008) first proposed an attribute chart (namely the *MON* chart) for monitoring the mean shifts of a process. This chart used the information of the magnitude of quality characteristic and the run length between two consecutive non-conforming samples. Their results show that the *MON* chart always excels the $\overline{X}$ chart and often outperforms the *CUSUM* chart based on the same inspection cost. After that, Wu, Khoo, Shu, and Jiang (2009) proposed a new np_x chart that also employed attribute inspection to monitor a process mean. The operational procedure of an np_x chart is as simple as that of a traditional *np* chart except that it uses the statistical warning limits to replace the specification limits for the classification of conforming or non-conforming units. As showed by Wu et al. (2009), the np_x chart usually outperforms the $\overline{X}$ chart on the basis of same inspection cost. As the np_x chart achieves higher detection effectiveness on mean shifts while retaining the operational simplicity of the attribute charts, some researchers have made efforts to improve the np_x chart in many aspects. For example, Sampaio, Ho, and de Medeiros (2014) combined np_x chart and $\overline{X}$ chart to monitor the process mean in a two-stage sampling. Their results show that the combined chart exhibits superior performance to the $\overline{X}$ control chart for a variety of sample sizes. Ho and Quinino (2013) proposed an np_s^2 chart which is similar to the np_x chart to monitor the variability of the process.

The above control charts using attribute inspection to monitor the mean shifts are all developed by fundamentally assuming that the sequence of process observations is statistically independent. This simple and traditional assumption is frequently used in most literature on SPC. However, this assumption is violated in some applications where the process variables are highly autocorrelated (Du & Lv, 2013; De Ketelaere, Rato, Schmitt, & Hubert, 2016; Simes, Leoni, & Costa, 2016). Therefore, many researchers have focused on the effect of autocorrelation property on the conventional control charts during the past decades. Chen and Huifen (2009) discussed the effect of autocorrelation on the Shewhart chart. Costa, Branco, and Machado (2011) also investigated the effect of the wandering behavior of the process mean on the performance of the variable parameter $\overline{X}$ chart and the double

* Corresponding author.
E-mail address: zhibzheng@gmail.com (Z. Zheng).

https://doi.org/10.1016/j.cie.2019.106081
Received 5 January 2019; Received in revised form 18 September 2019; Accepted 20 September 2019
Available online 23 September 2019

sampling $\overline{X}$ chart. Leoni and Costa (2015) investigated the performance of the T^2 control chart in the presence of autocorrelation. For more works in this area, see Vanhatalo and Kulahci (2015), Leoni, Costa, and Machado (2015) and so on. Since Alwan and Roberts (1988) proposed time-series model for statistical process control, the First Order Autoregressive $AR(1)$ model has been widely used for various control charts to accommodate autocorrelated processes due to its similarity and good performance on fitting the real-world production data. Franco, Costa, and Machado (2012) adopted $AR(1)$ model to describe the wandering behavior of the process mean. Nezhad, Fallah, and Niaki (2010) used a case study to compare the performance of the proposed method against the standard Shewhart, CUSUM, and EWMA charts based on the $AR(1)$ model. Franco, Celano, Castagliola, and Costa (2014) studied Shewhart control charts implementing skip sampling strategies for constructing subgroups based on the $AR(1)$ process. For more literature in this field, we refer the reader to He, Wang, Tsung, and Shang (2016) and Li, Mukherjee, Su, and Xie (2016) and so on.

As mentioned above, no method for evaluating the mean of the autocorrelated process by attribute inspection has been proposed. However, some manufacturing processes such as forging process, extruding process for the shaft, tubing and the filling process for plastic products and so on, are significantly found to be autocorrelated (Costa & Castagliola, 2011; Costa & Fichera, 2017).Using variable control chart to monitor the mean shifts of these types of processes is inappropriate and inefficient because the variable control chart with variable inspection like $\overline{X}$ chart needs to measure and record the exact value of quality characteristics of all samples which is time-consuming and high-cost. In contrast, the attribute inspection is more suitable for these cases because it only concerns that whether a unit is conforming (e.g., whether the diameters of the precision shaft or tubing within a region) rather than the actual value. Due to the simple implementation and relatively good performance of charts employing attribute inspection to monitor the process mean shifts for independent observations (like *MON* chart and np_x chart), it is potential and worth to further consider using the attribute inspection to detect the mean shifts of autocorrelated processes and investigate the effect of autocorrelation on the performance of this type of charts. In this paper, we propose an attribute chart to identify the mean of the autocorrelated processes whose distribution is assumed to follow the First Order Autoregressive ($AR(1)$) process. To optimally design the proposed chart, the average run length (*ARL*) is employed to measure the effectiveness of the proposed chart. Differing with related literature, we introduce a more tractable approach than Markov-chain approach to compute corresponding *ARL* by adopting the powerful Stein-Chen method.

The remainder of the paper is organized as follows: Section 2 describes the implementation of the proposed chart. Section 3 gives the analysis and optimal design of the proposed chart accommodating to autocorrelated process. Section 4 presents numerical experiments to compare the proposed chart with np_x chart and investigate the effectiveness and robustness of the proposed chart. Section 5 provides a realistic example to illustrate how to apply proposed chart to the manufacturing process. Finally, Section 6 concludes the paper and displays some idea about future work.

2. Implementation of the proposed chart

Among all of the attribute control charts, the procedure of the conventional *np* chart may be the simplest one for understanding and implementation in practice. Wu et al. (2009) first proposed np_x chart that employs the np-based procedure to monitor the process mean shifts for independent observations. The distinctive feature of the np_x chart is using the statistical warning limits to replace the specification limits for the classification of conforming or nonconforming units. Due to its simplicity, we use a similar procedure to detect the process mean shifts for autocorrelated processes. As shown in Fig. 1, the implemented procedure of the proposed chart is described as follows:

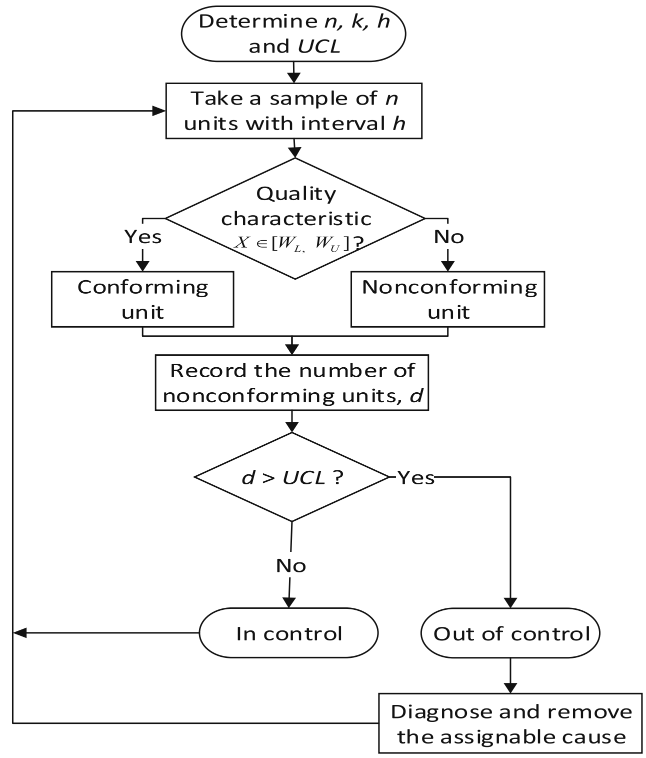

Fig. 1. The procedure of np_x control chart.

(1) Estimating in-control mean μ_0 and standard deviation σ_0, as well as correlation coefficient ρ fitted by regression analysis in Phase I.
(2) n units as a sample are taken and inspected with a sampling interval h.
(3) Each unit of a sample is classified as conforming item if its quality characteristic X lies in the interval between the lower warning limit W_L and upper warning limit W_U; otherwise, the item is classified as nonconforming. And calculating the number of nonconforming units within a sample d.
(4) If the number of nonconforming units d is greater than an upper control limit *UCL*, the process is considered statistically out of control; otherwise, the process is thought to be in control.

Note that the attribute inspection in step (2) only concerns that whether a unit is conforming (i.e., whether the quality characteristic $X \in [W_L, W_U]$) rather than the actual value of quality characteristic. It is also pointed out that as the autocorrelation is considered, the difference of implementation procedure between the proposed chart and the np_x chart is that the proposed chart need to estimate the parameters of $AR(1)$ model in the Phase I study. The parameter k is the warning limit coefficient of the lower warning limit W_L and upper warning limit W_U. The method to determine k, h, and *UCL* are explained in Section 3.2.

As introduced by Wu et al. (2009), this classification process can be simply accomplished by adopting a device, namely "Go/No Go" ring gage. As shown in Fig. 2, the calibrated dimension of the ring gage is designed equal to the upper warning limit W_U and lower warning limit W_L, respectively. An item is classified as conforming item if it passes through opening A but not opening B. In practice, this effective device

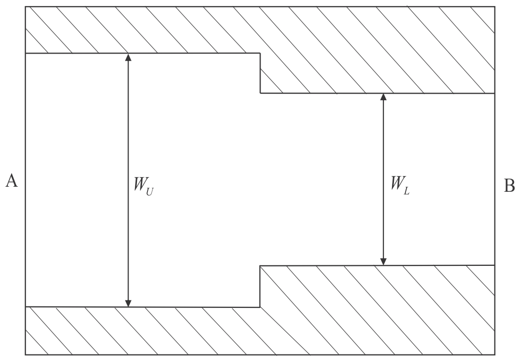

Fig. 2. "Go/No Go" Ring Gage.

is suitable for classifying the shaft and tubing which are usually produced from the forging or extruding processes. As Wardell, Moskowitz, and Plante (1994) give two practical examples to point out that forging and extruding processes are usually found to be autocorrelated, "Go/No Go" ring gage is also a powerful tool for our chart when the proposed chart is applied to these situations.

3. Analysis and design of the proposed chart for autocorrelated processes

3.1. Evaluation of statistical indices

In previous literature about using attribute inspection to monitor process mean shifts, the observations of a quality characteristic X are assumed to be independent, such as Wu and Jiao (2008) and Wu et al. (2009). In contrast, we assume that the observations of the quality characteristic X_i ($i = 1, 2, 3, ..., n$ represents the ith unit) within each sample of size n are autocorrelated and follow an identical normal distribution with known in-control mean μ_0 and standard deviation σ_0. Then, this process can be modeled by means of a First Order Autoregressive $AR(1)$ model, i.e.

$$X_i - \mu_0 = \rho(X_{i-1} - \mu_0) + \varepsilon_i \quad \text{for } i = 1, 2, ..., n \tag{1}$$

where $\rho \in (-1, 1)$ is the known $AR(1)$ parameter which is actually the correlation coefficient indicating relevance between observations of X_i and X_{i-1}. ε_i ($i = 1, 2, ..., n$) are i.i.d. normal random error variables and $\varepsilon_i \sim N(0, (1-\rho^2)\sigma_0^2)$ (Franco et al., 2014). Note that the observations of the quality characteristic between two consecutive samples are assumed to be independent. This is a common assumption in $AR(1)$ model, see Franco et al. (2014) and Chen and Huifen (2009).

For more details of this method, the reader is referred to Alwan and Roberts (1988). The reason why we adopt $AR(1)$ model to describe the autocorrelated observations is $AR(1)$ process has been encountered in many manufacturing systems, and $AR(1)$ model is also widely employed and investigated in lots of literature related to the control chart (see Introduction section).

After the assignable cause occurrence, the process variance remains unchanged, and the mean is supposed to shift from μ_0 to $\mu_1 = \mu_0 + \delta\sigma_0$ where δ is the magnitude of a mean shift in terms of σ_0. The lower warning limit W_L and the upper warning limit W_U are expressed as follows:

$$W_L = \mu_0 - k\sigma_0 \text{ and } W_U = \mu_0 + k\sigma_0 \tag{2}$$

where k is the warning limit coefficient.

Let p_i^j ($i = 1, 2, 3, ..., n; j = 0, 1$) be the probability that the ith unit within a sample is nonconforming, i.e., the observation of X_i in a sample is larger than W_U or smaller than W_L in state j (throughout this paper, we use $i = 1, 2, 3, ..., n$ represents the ith unit within a sample and $j = 0, 1$ indicates the process is in control and out of control respectively). In addition, let $\phi(\cdot)$ and $f(\cdot)$ be the cumulative distribution function (*cdf*) and probability density function (*pdf*) of the standard normal distribution respectively. Then, the expression of p_i^j is shown in Theorem 1.

Theorem 1. *Denote $\widehat{p}_i^j = P\{X_i > W_U\}$ by the probability that the observation of X_i in a sample is larger than W_U in state j and $\widetilde{p}_i^j = P\{X_i < W_L\}$ by the probability that the observation of X_i in a sample is smaller than W_L in state j. Then, $p_i^j = \widehat{p}_i^j + \widetilde{p}_i^j$ where $\widehat{p}_i^j$ and $\widetilde{p}_i^j$ are obtained from the recursion formulas as follows:*

(1) *when $i = 1$,*

$$\widehat{p}_1^j = 1 - \phi\left(\frac{W_U - \mu_j}{\sigma_0}\right) \text{ and } \widetilde{p}_1^j = \phi\left(\frac{W_L - \mu_j}{\sigma_0}\right); \tag{3}$$

(2) *when $2 \leqslant i \leqslant n$,*

$$\widehat{p}_i^j = \widehat{p}_{i-1}^j\widehat{A}_{i-1}^j + \widetilde{p}_{i-1}^j\widehat{B}_{i-1}^j + (1 - \widehat{p}_{i-1}^j - \widetilde{p}_{i-1}^j)\widehat{C}_{i-1}^j, \tag{4}$$

$$\widetilde{p}_i^j = \widehat{p}_{i-1}^j\widetilde{A}_{i-1}^j + \widetilde{p}_{i-1}^j\widetilde{B}_{i-1}^j + (1 - \widehat{p}_{i-1}^j - \widetilde{p}_{i-1}^j)\widetilde{C}_{i-1}^j, \tag{5}$$

where

$$\widehat{A}_{i-1}^j = \int_{W_U}^{+\infty}\left[1 - \phi\left(\left(W_U - \rho\left(X_{i-1} - \mu_j\right) - \mu_j\right)/\sqrt{1-\rho^2}\,\sigma_0\right)\right]f(X_{i-1})dX_{i-1},$$
$$\widetilde{A}_{i-1}^j = \int_{W_U}^{+\infty}\phi\left(\left(W_L - \rho\left(X_{i-1} - \mu_j\right) - \mu_j\right)/\sqrt{1-\rho^2}\,\sigma_0\right)f(X_{i-1})dX_{i-1},$$
$$\widehat{B}_{i-1}^j = \int_{-\infty}^{W_L}[1 - \phi((W_U - \rho(X_{i-1} - \mu_j) - \mu_j)/\sqrt{1-\rho^2}\,\sigma_0))]f(X_{i-1})dX_{i-1},$$
$$\widetilde{B}_{i-1}^j = \int_{-\infty}^{W_L}\phi((W_L - \rho(X_{i-1} - \mu_j) - \mu_j)/\sqrt{1-\rho^2}\,\sigma_0)f(X_{i-1})dX_{i-1},$$
$$\widehat{C}_{i-1}^j = \int_{W_L}^{W_U}\left[1 - \phi\left(\left(W_U - \rho\left(X_{i-1} - \mu_j\right) - \mu_j\right)/\sqrt{1-\rho^2}\,\sigma_0\right)\right]f(X_{i-1})dX_{i-1},$$
$$\widetilde{C}_{i-1}^j = \int_{W_L}^{W_U}\phi\left(\left(W_L - \rho\left(X_{i-1} - \mu_j\right) - \mu_j\right)/\sqrt{1-\rho^2}\,\sigma_0\right)f(X_{i-1})dX_{i-1}.$$

Proof. The proof of Theorem 1 is listed in the Appendix B. □

As shown in Theorem 1, the probability p_i^j depends on $\widetilde{p}_{i-1}^j$ and $\widehat{p}_{i-1}^j$ as a result of the autocorrelation property shown in Eq. (20). Since the classification of conforming or non-conforming units is a Bernoulli trial, we define Y_i^j ($i = 1, 2, 3, ..., n$) as a sequence of Bernoulli random variable for a fixed $j = 0, 1$ such that

$$Y_i^j = \begin{cases} 0 & W_L \leqslant X_i \leqslant W_U \\ 1 & X_i > W_U \text{ or } X_i < W_L, \end{cases}$$

then the total number of nonconforming units within a simple in state j is $d_j = \sum_{i=1}^n Y_i^j$ which is a sum of dependent Bernoulli random variables. As a result, it is difficult to derive the closed-form solution for the distribution of random variable d_j. Here, we introduce a more tractable method to compute this distribution by adopting the Stein-Chen method. And the following theorem gives the details.

Theorem 2. *If $n \to \infty$ and $\max_{1\leqslant i\leqslant n} p_i^j \to 0$, the total number of nonconforming units within a sample in state j, d_j, converges in distribution to a Poisson random variable with the mean $\lambda_j = E[d_j] = E[\sum_{i=1}^n Y_i^j] = \sum_{i=1}^n p_i^j$, i.e., the probability mass function (pmf) of d_j satisfies*

$$\lim_{\substack{n \to \infty \\ \max_{1 \leqslant i \leqslant n} p_i^j \to 0}} P\left(d_j = k\right) = \frac{\lambda_j^k}{k!} e^{-\lambda_j} \quad \left(k = 0, 1, 2, \ldots, n\right).$$

Proof. This can be intuitively obtained by the results of Arratia, Goldstein, and Gordon (1990). The Stein-Chen method is a general and powerful approach that approximates the distribution of an arbitrary sequence of dependent Bernoulli random variable by a Poisson distribution with the same mean. For more details of this method, the reader is referred to Stein (1972), Chen (1975) and Arratia et al. (1990). □

Note that the approximation showed in Theorem 2 is suitable for the case that the sample size n is relatively large and the fraction nonconforming of each sample p_i^j is relatively small. Next, let $P_j = P\{d_j > UCL\}$ be the probability that the total number of nonconforming units within a sample d is larger than UCL in state j, i.e., the probability that the control chart produces an out-of-control signal when the process is in state j. Based on the Theorem 2, for $j = 0$ or $j = 1$, the Stein-Chen approximation for the probability P_j is

$$\lim_{\substack{n \to \infty \\ \max_{1 \leqslant i \leqslant n} p_i^j \to 0}} P_j = 1 - \sum_{k=0}^{UCL} \frac{\lambda_j^k}{k!} e^{-\lambda_j}. \tag{6}$$

Therefore, the probability of a type I error α is

$$\alpha = P_0, \tag{7}$$

And the probability of type II error β is

$$\beta = 1 - P_1. \tag{8}$$

Denote by ARL_0 the in-control average run length, then

$$ARL_0 = \frac{1}{\alpha}. \tag{9}$$

And denote by ARL_1 the out-of-control average run length, then

$$ARL_1 = \frac{1}{1 - \beta}. \tag{10}$$

As it is difficult to derive the closed-form solution for ARL, we present a step-by-step description of the procedure for calculating ARL in the Table 1.

3.2. Optimal design of the proposed chart

The effectiveness of a control chart in detecting a process change is usually measured by the average run length (ARL) or average time to signal (ATS). Since the sampling interval of the proposed chart is constant, ARL is equivalent to ATS (Montgomery, 2007), and we choose ARL as a measurement to design our chart. In particularly, in-control average run length (ARL_0) characterizes a control chart's reliability whereas out-of-control average run length (ARL_1) measures the control chart's sensitivity to process excursions (Chen & Argon, 2007).

To design the proposed chart for autocorrelated processes, some parameters need to be predetermined: sample size (n), sampling interval (h), the allowed minimum ARL_0 (τ), the in-control process mean (μ_0), and standard deviation (σ_0), owing to considering correlation, ρ is also needed to be predetermined in Phase I. Among them, the values of n and h are usually selected depending on the available inspection resources. The allowed minimum ARL_0 is usually determined such that $\tau = 1/(1 + \phi(-3) - \phi(3)) = 370$ (Montgomery, 2007). In addition, the values of μ_0 and σ_0 are usually estimated based on the data obtained from the pilot runs. Then, the lower warning limit W_L, the upper warning limit W_U, and the upper control limit UCL are optimized by minimizing the ARL_1 while ARL_0 is equal to τ. Note that since the values of μ_0 and σ_0 are predetermined, to optimize W_L and W_U is equivalent to optimize k. The overall design is formulated by the following optimization model which can be achieved by the Genetic algorithm:

$$\min_{k,UCL} ARL_1 \tag{11}$$

$$\begin{aligned} s.t.\ & ARL_0 \geqslant \tau \\ & k > 0 \\ & UCL > 0,\ UCL \in N^* \end{aligned}$$

Table 1
Step-by-step description of the procedure for calculating ARL (given k and UCL).

Set μ_0, σ_0, δ, n, k and UCL	
Compute $\hat{p}_1^0, \tilde{p}_1^0, \hat{p}_1^1$ and $\tilde{p}_1^1$	% computed through Theorem 1
Compute $p_1^0 = \hat{p}_1^0 + \tilde{p}_1^0$ and $p_1^1 = \hat{p}_1^1 + \tilde{p}_1^1$	
Set $\lambda_0 = p_1^0$ and $\lambda_1 = p_1^1$	
[cycle i] **For** $i = 2$ **To** n **step** 1	
Compute $\hat{p}_i^0, \tilde{p}_i^0, \hat{p}_i^1$ and $\tilde{p}_i^1$	% computed through Eqs. (4) and (5)
Compute $p_i^0 = \hat{p}_i^0 + \tilde{p}_i^0$ and $p_1^1 = \hat{p}_i^1 + \tilde{p}_i^1$	
Compute $\lambda_0 = \lambda_0 + p_i^0$ and $\lambda_1 = \lambda_1 + p_i^1$	
Next[cycle i]	
Compute P_0 and P_1	% computed through Eq. (6)
Compute $ARL_0 = \frac{1}{P_0}$ and $ARL_1 = \frac{1}{P_1}$	
Stop	

4. Numerical analysis

In this section, we compare the statistical performance of the proposed control chart with np_x chart proposed by Wu et al. (2009) for monitoring a set of autocorrelated data and carry out a sensitivity analysis of the proposed control chart.

4.1. The performance of the Stein-Chen approximation method

In this paper, we proposed a more tractable approach to compute the average run length (ARL) by adopting the Stein-Chen method. In previous literature, a similar problem is usually solved by some complicated methods like constructing a Markov chain which adds an extra degree of difficulty for operators. In this subsection, we first do some numerical experiments to investigate the performance of the Stein-Chen approximation method.

Arratia et al. (1990) proved that there is an error bound for the Stein-Chen approximation. Details can be found in Arratia et al. (1990). We briefly introduce the error bound of this approximation method as follows:

Before introducing the error bound, we first give some definitions. Write $f(X)$ for the law or distribution of X, for a real valued function h defined on the support of X and Y, let $\left\|h\right\| = \sup_k \left|h(k)\right|$. Define the total variation distance between X and Y, one may write

$$\left\|f(X) - f(Y)\right\| = 2\sup_A \left|P\left(X \in A\right) - P\left(Y \in A\right)\right|. \tag{12}$$

Let I be a finite or countable index set. For any $i \in I$, let Y_i be a Bernoulli random variable. For each $i \in I$, we suppose the set $B_i \subset I$ with $i \in B_i$ as a dependent neighborhood of i, then for any $i, j \in B_i$, Y_i and Y_j are dependent.

Furthermore, define

$$b_1 = \sum_{i \in I} \sum_{j \in B_i} p_i p_j, \tag{13}$$

$$b_2 = \sum_{i\in I}\sum_{i\neq j\in B_i} p_{ij},\ p_{ij} = E\left[Y_iY_j\right] = P\left\{Y_iY_j = 1\right\} = P\left\{Y_i = 1,\ Y_j = 1\right\}, \tag{14}$$

$$b_3 = \sum_{i\in I} E\left[E\left[Y_i - p_i\middle|Y_j: j\notin B_i\right]\right], \tag{15}$$

where b_1 is the neighborhood size, b_2 is the expected number of neighbors of a given occurrence and b_3 measures the dependence between an event and the number of occurrences outside its neighborhood.

Theorem 3. *Let $W = \sum_{i\in I} Y_i$ be the number of occurrence of some dependent events, and let Z be a poisson random variable with mean $E[Z] = E[W] = \lambda$. Then*

$$\begin{aligned}\|f(W) - f(Z)\| &\leqslant 2\left[\left(b_1 + b_2\right)\frac{1-e^{\lambda}}{\lambda} + b_3\left(1\wedge 1.4\lambda^{-0.5}\right)\right]\\ &\leqslant 2(b_1 + b_2 + b_3).\end{aligned} \tag{16}$$

By Theorem 3, an error bound for the approximation is

$$\|f(W) - f(Z)\| \leq 2(b_1 + b_2 + b_3). \tag{17}$$

In particular, when $B_i = I$, then $b_3 = 0$, Eq. (6) is reduced to

$$\|f(W) - f(Z)\| \leq 2(b_1 + b_2). \tag{18}$$

Then, for our model, an error bound can be expressed by

$$\left|\sum_{i=0}^{UCL} f(W) - \sum_{i=0}^{UCL} f(Z)\right| \leq 2\left(b_1 + b_2\right). \tag{19}$$

It is obvious that the smaller the value of error bound, the better the performance of the approximation. To investigate the effect of n on the error bound of the probability P_j in the Eq. (6). We calculate error bounds for a series of sample size n. The results can be seen in Table 2.

As can be seen from Table 2, when n starts from 10, the error bound is relatively small, and as n increases, the approximation performs better.

4.2. Comparison studies

As Wu et al. (2009) also employed similarly *np*-based procedure to monitor the process mean shifts for independent observations, we compare the statistical performance of the proposed control chart based on autocorrelated processes (referred to as "$AR - np_x$ chart" throughout) with Wu et al.'s (2009) np_x chart (referred to as "$ID - np_x$ chart" throughout) in this subsection. Without loss of generality, we consider the situation where $\mu_0 = 0$, $\sigma_0 = 1$ and $\tau = 370$. Both positive and negative correlation coefficients are considered, i.e., $\rho \in \{-0.9, -0.5, -0.1, 0.1, 0.5, 0.9\}$. In addition, the other two parameters are set to vary at several levels: the magnitude of a mean shift $\delta \in \{0, 0.5, 1, 1.5\}$ and the sample size $n \in \{10, 15, 20\}$. Now, we introduce following steps to conduct the comparison between two charts:

Table 2
Error bound for different n.

sample size	error bound
10	0.0217
15	0.0135
20	0.0097
30	0.0062
50	0.0039
60	0.0029

Table 3
The comparison results of two control charts when $\rho < 0$.

ρ	δ	n	$ID - np_x$ chart			$AR - np_x$ chart		
			UCL	k	ARL	UCL	k	ARL
−0.9	0	10	5	1.3725	14429.00	7	0.2742	370.04
		15	4	1.8149	10629.00	6	0.8768	370.20
		20	4	1.9552	10084.00	5	1.3020	370.26
	0.5	10	6	1.1758	13101.00	6	0.5788	357.65
		15	3	2.0426	1291.20	5	1.1172	267.21
		20	3	2.1688	1132.80	4	1.5447	181.51
	1	10	6	1.1758	8832.80	5	0.8491	186.58
		15	5	1.6276	945.32	5	1.1175	136.99
		20	5	1.7820	604.66	3	1.8271	31.49
	1.5	10	5	0.8494	3162.70	5	0.8491	111.32
		15	5	1.6276	208.95	4	1.3813	32.51
		20	4	1.9554	47.72	2	2.1816	6.46
-0.5	0	10	5	1.3725	882.82	7	0.6838	370.00
		15	4	1.8149	701.33	7	1.1153	370.21
		20	4	1.9552	690.68	6	1.5061	370.85
	0.5	10	6	1.1758	754.61	6	0.9839	295.72
		15	3	2.0426	145.61	4	1.7353	129.07
		20	3	2.1688	120.91	3	2.1194	88.93
	1	10	6	1.1758	325.09	5	1.2435	97.93
		15	5	1.6276	61.86	4	1.7353	25.96
		20	5	1.7820	33.54	4	1.8836	16.01
	1.5	10	5	0.8494	41.17	4	1.5044	22.79
		15	5	1.6276	22.89	2	2.3099	3.74
		20	4	1.9554	5.98	3	2.1194	3.47
-0.1	0	10	5	1.3725	473.50	6	1.0818	370.03
		15	4	1.8149	393.74	6	1.4081	370.25
		20	4	1.9552	393.57	5	1.7611	370.17
	0.5	10	6	1.1758	345.85	5	1.3354	172.69
		15	3	2.0426	81.55	2	2.3506	78.66
		20	3	2.1688	69.10	2	2.4568	68.32
	1	10	6	1.1758	135.71	4	1.5853	30.36
		15	5	1.6276	24.23	5	1.6003	22.36
		20	5	1.7820	13.24	4	1.9484	9.20
	1.5	10	5	0.8494	27.72	4	1.5853	13.16
		15	5	1.6276	9.88	4	1.8074	5.28
		20	4	1.9554	2.95	3	2.1707	2.13

Step 1. For $AR - np_x$ chart, we use our model proposed in Section 3 and the above autocorrelated data directly to obtain the optimal k, UCL and corresponding ARL_1 (or ARL_0 when $\delta = 0$);
Step 2. For $ID - np_x$ chart, we use Wu et al.'s (2009) model to obtain optimal k_1 and UCL_1 except that the correlation coefficients is considered to be zero, i.e., $\rho = 0$. Next, for the same autocorrelated data set, we substitute the optimal k_1 and UCL_1 into Eq. (10) (or Eq. (9) when $\delta = 0$) to obtain the corresponding ARL_1 (or ARL_0 when $\delta = 0$);
Step 3. Compare the effectiveness of two control charts in detecting the same autocorrelated process change through their ARL_1 (or ARL_0 when $\delta = 0$).

The idea behind the above method is that whether the $ID - np_x$ chart performs as well as $AR - np_x$ chart when it ignores the correlation properties of data. The results are shown in the Tables 3 and 4. Particularly, the column of ARL represents ARL_0 when $\delta = 0$, otherwise it represents ARL_1.

In Table 3, the ARL_0 (when $\delta = 0$) of $ID - np_x$ chart is always larger than that of $AR - np_x$ chart when the correlation is negative. In Table 4, the ARL_1 (when $\delta \neq 0$) of $ID - np_x$ chart is always smaller than that of $AR - np_x$ chart when the correlation is positive. These observations ostensibly show that $ID - np_x$ chart may outperform $AR - np_x$ chart in some situations. However, this is found to be invalid when we completely observe the data of Tables 3 and 4. Next, we draw some figures based on the data of Tables 3 and 4 to intuitively interpret our findings.

As shown in the (a_1) and (a_2) of Fig. 3, when the correlation

Table 4
The comparison results of two control charts when $\rho > 0$.

ρ	δ	n	$ID - np_x$ chart			$AR - np_x$ chart		
			UCL	*k*	*ARL*	*UCL*	*k*	*ARL*
0.1	0	10	5	1.3725	104.17	7	0.7847	370.44
		15	4	1.8149	67.57	7	1.2184	370.16
		20	4	1.9552	56.18	5	1.7611	370.17
	0.5	10	6	1.1758	34.22	6	1.0818	198.06
		15	3	2.0426	16.95	5	1.6003	97.10
		20	3	2.1688	12.34	4	1.9484	66.70
	1	10	6	1.1758	5.03	5	1.3354	41.66
		15	5	1.6276	2.21	6	1.4081	26.73
		20	5	1.7820	1.60	3	2.1707	6.40
	1.5	10	5	0.8494	0.57	4	1.5853	10.34
		15	5	1.6276	0.66	3	2.0469	2.75
		20	4	1.9554	0.57	2	2.4589	1.58
0.5	0	10	5	1.3725	2.69	6	0.9839	370.13
		15	4	1.8149	1.51	5	1.5155	370.11
		20	4	1.9552	1.27	5	1.6842	370.21
	0.5	10	6	1.1758	2.10	5	1.2435	92.57
		15	3	2.0426	0.81	4	1.7353	56.53
		20	3	2.1688	0.64	3	2.1194	49.12
	1	10	6	1.1758	1.19	5	1.2435	21.85
		15	5	1.6276	0.63	3	1.9894	6.03
		20	5	1.7820	0.55	2	2.4226	5.20
	1.5	10	5	0.8494	0.53	4	1.5044	6.45
		15	5	1.6276	0.53	3	1.9896	1.86
		20	4	1.9554	0.50	4	1.8836	1.50
0.9	0	10	5	1.3725	1.02	5	0.8491	370.11
		15	4	1.8149	1.00	4	1.3813	370.09
		20	4	1.9552	1.00	5	1.3020	370.26
	0.5	10	6	1.1758	0.53	6	0.5788	38.87
		15	3	2.0426	0.50	5	1.1172	12.90
		20	3	2.1688	0.50	5	1.3020	9.30
	1	10	6	1.1758	0.53	4	1.1436	4.84
		15	5	1.6276	0.50	3	1.6845	2.36
		20	5	1.7820	0.50	3	1.8270	1.77
	1.5	10	5	0.8494	0.50	3	1.4779	2.06
		15	5	1.6276	0.50	2	2.0594	1.01
		20	4	1.9554	0.50	2	2.1813	0.81

coefficient is negative, although the ARL_0 of $ID - np_x$ chart is larger than that of $AR - np_x$ chart, the ARL_1 of $ID - np_x$ chart is also too large resulting in a high probability of type II error. Furthermore, as illustrated in the (a_3) and (a_4) of Fig. 3, when the correlation coefficient is positive, the ARL_1 of $ID - np_x$ chart is smaller than that of $AR - np_x$ chart, however, the ARL_1 of $ID - np_x$ chart is also too small (even closes to zero with a high autocorrelation coefficient) which leads to a high probability of type I error. From the above description, we summarize the following observation.

Observation 1. When the $AR - np_x$ chart is employed to detect the autocorrelated processes, the corresponding ARL_0 is relatively stable and always keeps around 370 (i.e., the allowed minimum ARL_0) while the corresponding ARL_1 is relatively small. In contrast, if the $ID - np_x$ chart which ignores the correlation properties is used to detect the same processes, the corresponding ARL_0 and ARL_1 can not be traded off well.

In other words, the Observation 1 indicates that if there exists autocorrelated data, and we continue to employ $ID - np_x$ chart to monitor the mean of data, it will cause a false alarm or a missed alarm consistent with the results of Xu and Huang (2014), this statistically shows that ARL_0 is too large or ARL_1 is too small. Our control chart can solve this problem very well because our model considers autocorrelation, the control limits are calculated based on the autocorrelation coefficient, so both ARL_0 and ARL_1 are normal. If we tune the $ID - np_x$ chart to have an equal ARL_0 of $AR - np_x$ chart, which will terribly have a bad effect on the performance of these two charts. Therefore, ARL_0 of the two charts are of big difference, and it is impossible to tune the $ID - np_x$ chart to have an equal ARL_0 of $AR - np_x$ chart. Furthermore, from (a_2) and (a_4) of Fig. 3, we make the following observation.

Observation 2. (1) When $\rho < 0$ and the correlation is high, the gap between the ARL_1 of two charts is bigger;

(2) When $\rho > 0$ and the correlation is low, the gap between the ARL_1 of two charts is bigger.

The Observation 2 shows that although the $AR - np_x$ always outperforms $ID - np_x$ chart regardless of the correlation, relatively speaking, the $AR - np_x$ chart performs better when the observations of the quality characteristic is highly negative correlation or lowly positive correlation. Figs. 4 and 5 further confirm the Observation 1 that using $ID - np_x$ chart to monitor the autocorrelated processes causes a false-alarm risk regardless of the change of the shifts and sample size. Particularly, from (b_4), (c_2) and (c_4), we find that the $AR - np_x$ chart relatively performs better and we summarize these cases as the following observations.

Observation 3. (1) When the correlation is positive, and shifts are small, the gap between the ARL_1 of two charts is bigger;

(2) When the sample size is small, the gap between the ARL_1 of two charts is bigger.

Overall, we conclude that the $AR - np_x$ chart proposed in this paper generally outperforms $ID - np_x$ chart proposed by Wu et al. (2009) in detecting the mean shifts when considering the condition with an autocorrelation coefficient.

4.3. The performance of the proposed chart when data deviates from $AR(1)$ process

As the simplicity and wide application of the $AR(1)$ model, lots of literature have dealt with autocorrelated data in production process based on this model. However, in reality, the production data may not fit $AR(1)$ model well. Therefore, it is interesting to investigate the performance of the proposed chart when data deviates from $AR(1)$ process.

When an autocorrelated process that deviates from the $AR(1)$ model, we consider it fits the other model like the $AR(2)$ model. The reason why we choose the $AR(2)$ model as an example is that it has been also used in a wide variety of applications (Singh, 2013). The $AR(2)$ model is shown as follows:

$$X_i - \mu_0 = \phi_1(X_{i-1} - \mu_0) + \phi_2(X_{i-2} - \mu_0) + \varepsilon_i \quad \text{for } i = 1, 2, \ldots, n, \tag{20}$$

where $\phi_2 \in (-1, 1)$ and $\phi_1 \pm \phi_2 < 1$, besides, ε_i $(i = 1, 2, \ldots, n)$ are a sequence of independent identically distributed (i.i.d.) random variables that $\varepsilon_i \sim N(0, \sigma_\varepsilon^2)$. Note $\sigma_X^2 = \gamma_0\sigma_\varepsilon^2$ in which $\gamma_0 = \frac{1-\phi_2}{(1+\phi_2)(1-\phi_2+\phi_1)(1-\phi_2-\phi_1)}$.

In order to analyze the performance of the $AR - np_x$ chart for an autocorrelated process that deviates from an $AR(1)$ model, we design an experiment in the following steps:

Step 1. We set a series of basic parameters for $AR(2)$ model $\{\mu_0, \sigma_0, \delta, n\} = \{0, 1, 0.5, 100\}$. In order to investigate the results under different data structures, we set $\phi_1 \in \{0.1, 0.2, 0.3\}$ and $\phi_2 \in \{0.01, 0.04, 0.09\}$;

Step 2. Using Monte Carlo simulation to generate data set based on the basic parameters of the $AR(2)$ model. And estimating the correlation coefficient $\hat{\rho}$ of the $AR(1)$ model by using this generated

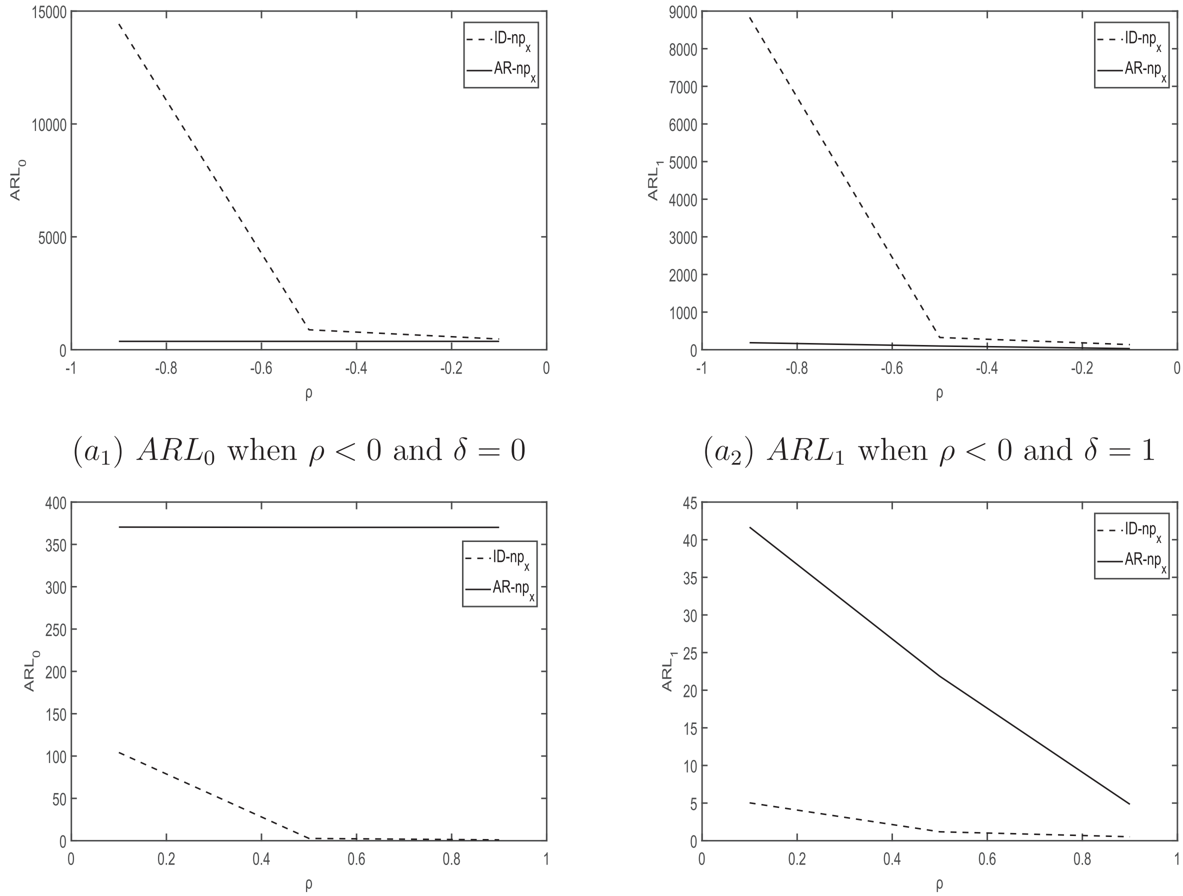

(a_1) ARL_0 when $\rho < 0$ and $\delta = 0$

(a_2) ARL_1 when $\rho < 0$ and $\delta = 1$

(a_3) ARL_0 when $\rho > 0$ and $\delta = 0$

(a_4) ARL_1 when $\rho > 0$ and $\delta = 1$

Fig. 3. The comparison of the *ARL* of two charts with varying correlation coefficient ρ (n = 15).

data set;

Step 3. Using estimated $\hat{\rho}$ of $AR(1)$ model to design optimal parameters k^* and UCL^* of $AR - np_x$ chart and obtaining the corresponding ARL_0 and ARL_1. Next, we apply the above optimal $AR - np_x$ chart based on $AR(1)$ model to monitor the generated data based on the basic parameters of $AR(2)$ model and calculate the corresponding $\widehat{ARL_0}$ and $\widehat{ARL_1}$;

Step 4. Finally, comparing ARL_0, ARL_1 with $\widehat{ARL_0}$ and $\widehat{ARL_1}$ respectively to investigate the performance of the proposed chart when data doesn't fit $AR(1)$ process;

As is shown in Table 5, the estimated $\hat{\rho}$ increases as ϕ_1 or ϕ_2 increases. Although the parameter of $AR(2)$ model ϕ_1 or ϕ_2 has a big change, the variation of the estimated $\hat{\rho}$ ranges from 3% to 6%, which results in a small change for ARL_1 of $AR(1)$ model. When the optimal $AR - np_x$ chart based on $AR(1)$ model is applied to monitor the generated data based on the basic parameters of AR(2) model, both $\widehat{ARL_0}$ and $\widehat{ARL_1}$ are sensitive to ϕ_1 and ϕ_2 and decreasing rapidly when ϕ_1 or ϕ_2 increases. Surprisingly, when both ϕ_1 and ϕ_2 are small, there is little difference between ARL_1 and $\widehat{ARL_1}$, which indicates the proposed chart may be efficient on monitoring the mean shifts in this situation even the autocorrelated processed deviates from an $AR(1)$ model.

In addition, in order to compare the performance of $ID - np_x$ chart with $AR - np_x$ chart when the autocorrelated processed deviates from an $AR(1)$ model, we adopt similar experiment to apply optimal $ID - np_x$ chart based on the independent process to monitor the generated data based on the basic parameters of $AR(2)$ model.

In Table 6, $\widehat{ARL_0}$ and $\widehat{ARL_1}$ represent the corresponding ARL_0 and ARL_1 when using optimal $ID - np_x$ chart to monitor the generated data based on the basic parameters of $AR(2)$ model. From Table 3, since the correlation is not considered, the ARL_0 and ARL_1 of the $ID - np_x$ chart remain unchanged regardless of the variation in the estimated $\hat{\rho}$. Owing to the optimal parameters are fixed, when optimal $ID - np_x$ chart is applied to monitor the $AR(2)$ model, the variational ranges of $\widehat{ARL_0}$ and $\widehat{ARL_1}$ are relatively small. Compared with the $ID - np_x$ chart, when the optimal $AR - np_x$ chart based on $AR(1)$ model is applied to monitor the generated data based on the $AR(2)$ model, the corresponding $\widehat{ARL_0}$ is larger as the correlation is small. This can reduce the type I error. Moreover, the corresponding $\widehat{ARL_1}$ drops quickly as $\hat{\rho}$ changes, which is also conducive to reduce the type II error.

All in all, if the autocorrelated process deviates from an $AR(1)$ model, it has an effect on the performance of the proposed chart, but this effect is relatively small when the correlation is small. Moreover, the proposed chart performs better than $ID - np_x$ chart when monitoring the same data set. Therefore, it is better to estimate whether the structure of the data fits $AR(1)$ model before using the proposed chart.

4.4. Sensitivity analysis

In this subsection, we first investigate the robustness of the proposed chart when the predetermined parameters are estimated

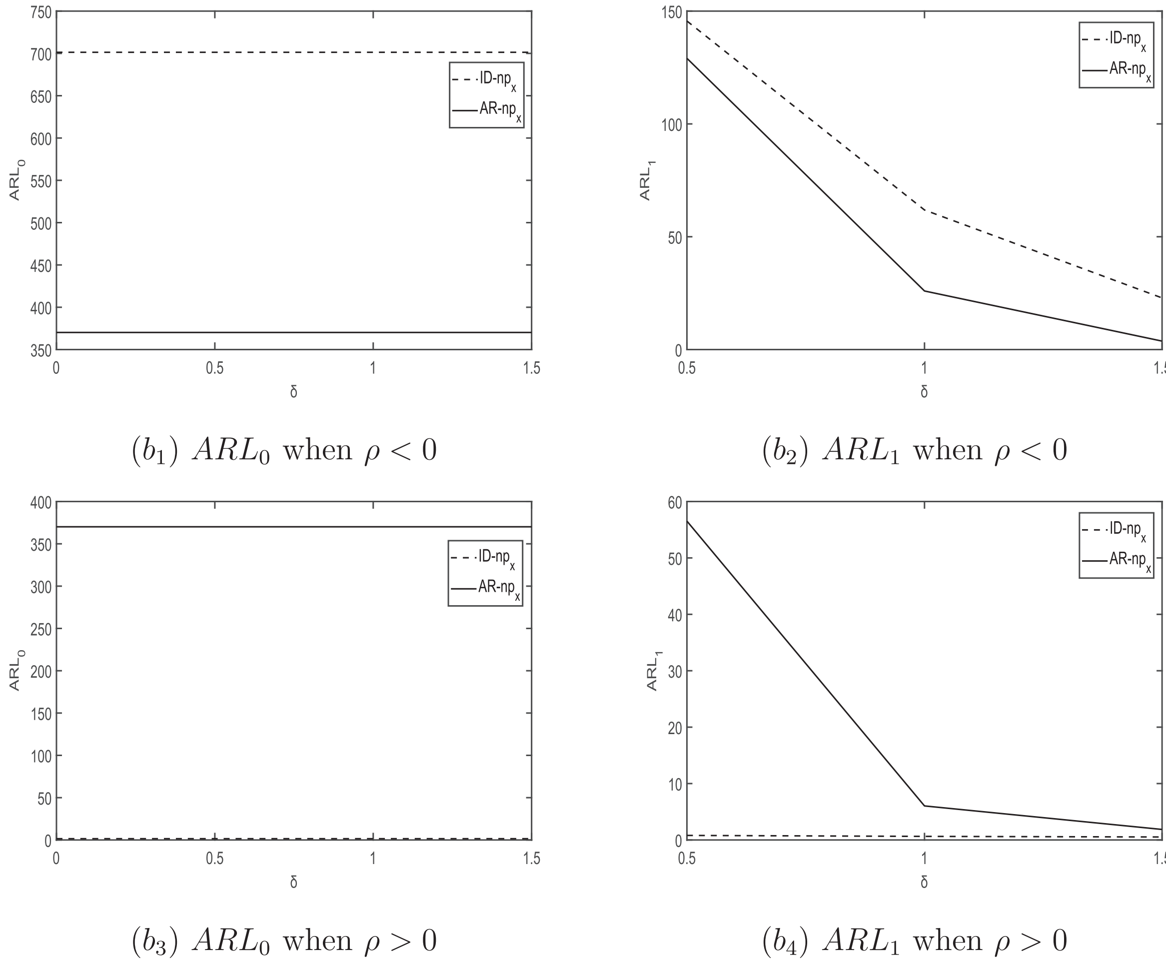

Fig. 4. The comparison of the *ARL* of two charts with varying shifts δ ($n = 15$).

inaccurately. Without loss of generality, we consider the situation where $\mu_0 = 0$, $\sigma_0 = 1$, and $\tau = 370$. The experiments are provided with different schemes which consist of the following benchmarks (represent true value of the parameter): the process mean shift $\delta \in \{0.1, 0.5\}$ and the correlation coefficient $\rho \in \{-0.5, -0.1, 0.1, 0.5\}$. Based on the benchmarks, the estimated value of every parameter is supposed to deviate from true value and is chosen as fluctuating up and down ten percent. Then, we observe how the change of each parameter effects on the ARL_1 of the proposed chart. The results are shown in the Tables 7–9. The numbers in brackets are the proportion of the change of ARL_1 which are computed as $\Delta = (ARL_1 - ARL_1^b)/ARL_1^b$ where ARL_1^b is the corresponding value of the benchmark.

In Tables 7 and 8, the high correlation and low correlation situations are investigated respectively with the sample size $n = 10$. As shown in Table 7, when the correlation is low, all the absolute value of the proportion is within 1.5% and the proposed chart is fairly robust regardless of process mean shifts. Particularly, the performance is better in case of small mean shifts. In Table 8, for the case of high correlation, the proportion of the change of ARL_1 is still relatively small when the correlation is positive except that it rises to 14.43% when the shift of process mean is zero. However, the proportion of the change of ARL_1 is relatively large in the case of a highly negative correlation. Overall, the proposed chart is relatively robust in the various levels of positive correlation and lowly negative correlation.

Similarly, in Table 9, two levels of the process mean shifts are considered as benchmarks respectively with the sample size $n = 10$. It demonstrates that when the shifts are relatively small (see the first three columns), the proposed chart is robust to the shifts in different parameters. When the shifts gradually increase (see the last three columns), the robustness of the proposed chart decreases and the ARL_1 fluctuates greatly, especially when the correlation is high. For example, the proportion of the change of ARL_1 rises to 21.49% when the correlation is 0.5. This indicates that the process mean shifts are worth paying more efforts to estimate in this case due to their significant effects on the performance of the proposed chart.

5. An industry example

In this section, we adopt industry data from a yogurt cup filling process to illustrate the use of the proposed chart. This data is utilized by Costa and Castagliola (2011) which consists of 200 observations of the weight of yogurt cup. The reason why we adopt this example to illustrate the use of our chart is: (1) Costa and Castagliola (2011) showed that a large database of yogurt cup weights satisfactorily fits to an $AR(1)$ model; (2) The attribute inspection for the weight of yogurt cup is also simple to accomplish.

The data collected by Costa and Castagliola (2011) is shown in Table 11 in the Appendix A. It consists of 20 samples with size $n = 10$

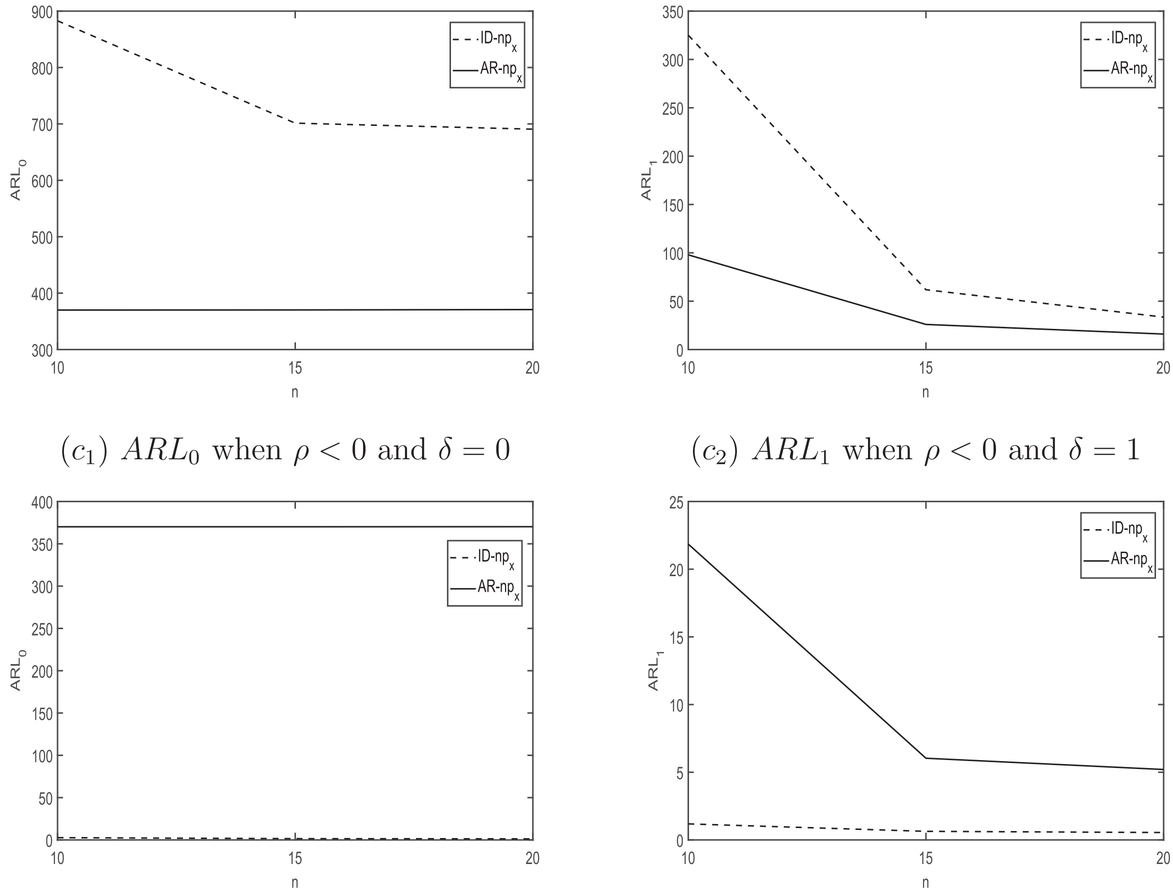

(c_1) ARL_0 when $\rho < 0$ and $\delta = 0$

(c_2) ARL_1 when $\rho < 0$ and $\delta = 1$

(c_3) ARL_0 when $\rho > 0$ and $\delta = 0$

(c_4) ARL_1 when $\rho > 0$ and $\delta = 1$

Fig. 5. The comparison of the *ARL* of two charts with varying sample size *n*.

and sampling interval $h = 1$. The proposed chart is based on attribute inspection which only concerns whether the weight of the yoghurt cup is conforming. In this example, the classification process of the yogurt cup could be accomplished by using a balance which is similar to the "Go/No Go" ring gage. A yoghurt cup is considered unapproved if its weight is greater than a weight equalling to W_U or less than a weight equalling to W_L. This only needs to observe the shift of balance rather than precisely read and record measure data. This classification process is intuitively shown in Fig. 6.

Therefore, when the proposed chart is employed to monitor the same processes, the original data set based on variable inspection (shown in Table 11 in Appendix A) could be transformed into Table 10 in which '–' represents the unit is conforming and the value of number represents the total number of nonconforming unit within a sample.

Based on Table 10, the scatter plots of $AR - np_x$ chart are shown in Fig. 7. From (b2) of Fig. 7, we find that the production process is out of control in the eleventh sample. This indicates that the mean of the yogurt cup filling process has shifted.

Table 5
The performance of the proposed chart when the autocorrelated processed deviates from an $AR(1)$ model.

ϕ_1	ϕ_2	$\hat{\rho}$	optimal parameters		$AR(1)$ model		AR(2) model	
			UCL	k	ARL_0	ARL_1	$\widehat{ARL_0}$	$\widehat{ARL_1}$
0.1	0.01	0.086	8	2.1666	370.4532	18.9438	304.878	17.9216
	0.04	0.089	7	2.1665	370.4435	18.8999	293.2551	17.262
	0.09	0.093	9	2.09	370.0793	18.6883	255.7545	15.248
0.2	0.01	0.185	7	2.3435	370.0241	18.1612	148.5884	9.5857
	0.04	0.191	7	2.2465	370.5272	18.1029	129.8701	9.1525
	0.09	0.204	7	2.2456	370.5174	17.94	93.633	7.1086
0.3	0.01	0.282	8	2.1524	370.5276	16.1339	45.2489	4.9855
	0.04	0.292	8	2.1512	370.5054	15.9839	42.1941	4.6177
	0.09	0.306	8	2.1494	370.2969	15.7665	26.738	3.4063

Table 6
The comparison between the performance of $ID-np_x$ chart and $AR-np_x$ chart when the autocorrelated processed deviates from an $AR(1)$ model.

ϕ_1	ϕ_2	$\hat{\rho}$	optimal parameters		independent process		AR(2) model	
			UCL	k	$\overline{ARL_0}$	$\overline{ARL_1}$	$\widetilde{ARL_0}$	$\widetilde{ARL_1}$
0.1	0.01	0.086	6	2.3543	370.2928	17.7921	285.7143	15.2978
	0.04	0.089					232.5581	13.93
	0.04	0.089					196.0784	13.3504
0.2	0.01	0.185					181.8182	10.7613
	0.04	0.191					138.8889	9.8413
	0.04	0.204					116.8224	8.8345
0.3	0.01	0.282					60.5694	6.2801
	0.04	0.292					50.5817	5.9562
	0.04	0.306					37.3692	5.0264

Table 7
Sensitivity analysis of ρ (low correlation).

δ	ρ					
	$-0.11(-10\%)$	-0.1	$-0.09(+10\%)$	$0.09(-10\%)$	0.1	$0.11(+10\%)$
0	$371.0896(+0.29\%)$	370.0331	$368.134(-0.51\%)$	$369.4349(-0.27\%)$	370.4382	$371.5536(+0.30\%)$
0.5	$174.5742(+1.09\%)$	172.6948	$170.8868(-1.05\%)$	$199.182(+0.57\%)$	198.0629	$196.9853(-0.54\%)$
1	$30.7978(+1.43\%)$	30.3641	$29.9418(-1.39\%)$	$42.209(+1.31\%)$	41.6617	$41.125(-1.29\%)$
1.5	$13.3308(+1.32\%)$	13.1575	$12.988(-1.29\%)$	$10.4533(+1.14\%)$	10.3358	$10.2203(-1.12\%)$

In this example, the proposed chart uses the same data (i.e., the same sample size) to yield the same conclusion (i.e., the production process is found to be out of control in the eleventh sample) as the variable chart proposed by Costa and Castagliola (2011). However, comparing with the variable inspection adopted by the chart of Costa and Castagliola (2011), the attribute inspection is commonly believed to be much simpler and less time-consuming especially when some time-saving measuring instruments are implemented, for example, "Go/No Go" ring gage (Montgomery, 2007). Therefore, the sample sizes of the attribute charts are usually much larger than that of the variable charts on the basis of same inspection cost (Wu et al., 2009). Based on the above, the proposed chart may use a larger sample size and/or sampling frequency based on equal inspection cost, and therefore has a higher or substantially higher detection effectiveness than the one proposed by Costa and Castagliola (2011).

6. Conclusion and discussion

In this paper, an attribute chart is proposed to monitor the mean of the autocorrelated processes. To design the proposed chart, the distribution of observations is supposed to follow the First Order Autoregressive ($AR(1)$) process. The average run length (ARL) is

Table 8
Sensitivity analysis of ρ (high correlation).

δ	ρ					
	$-0.55(-10\%)$	-0.5	$-0.45(+10\%)$	$0.45(-10\%)$	0.5	$0.55(+10\%)$
0	$407.1926(+10.05\%)$	370.0039	$341.2246(-7.78\%)$	$329.9736(-10.85\%)$	370.1253	$423.5482(+14.43\%)$
0.5	$339.7268(+14.88\%)$	295.7155	$262.551(-11.22\%)$	$91.8552(-0.77\%)$	92.5688	$93.7212(+1.24\%)$
1	$112.6496(+15.03\%)$	97.9306	$86.3367(-11.84\%)$	$23.1544(+5.95\%)$	21.8537	$20.6142(-5.67\%)$
1.5	$25.3776(+11.35\%)$	22.7918	$20.6556(-9.37\%)$	$6.7707(+4.96\%)$	6.4505	$6.1451(-4.73\%)$

Table 9
Sensitivity analysis of δ.

ρ	δ					
	$0.09(-10\%)$	0.1	$0.11(+10\%)$	$0.45(-10\%)$	0.5	$0.55(+10\%)$
-0.5	$363.0468(+0.42\%)$	361.52	$359.8444(-0.46\%)$	$307.1433(+3.86\%)$	295.7155	$284.1883(-3.90\%)$
-0.1	$354.5052(+0.89\%)$	351.3808	$347.4656(-1.11\%)$	$194.9693(+12.90\%)$	172.6948	$152.5494(-11.67\%)$
0.1	$349.37(+1.31\%)$	344.846	$339.9385(-1.42\%)$	$218.2927(+10.21\%)$	198.0629	$179.5066(-9.37\%)$
0.5	$343.5711(+1.70\%)$	337.8352	$331.6488(-1.83\%)$	$112.4608(+21.49\%)$	92.5688	$76.5369(-17.32\%)$

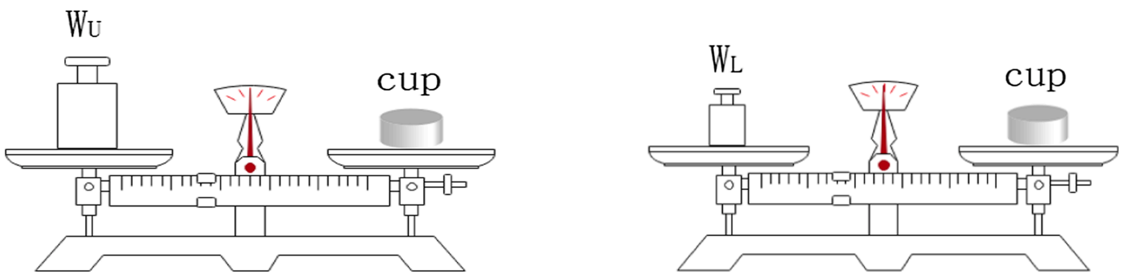

(a_1) Comparing with W_U (a_2) Comparing with W_L

Fig. 6. The classification process of the weight of yogurt cup.

Table 10
The data set for the classification process of the weight of yogurt cup.

Sample number	X_1	X_2	X_3	X_4	X_5	X_6	X_7	X_8	X_9	X_{10}	d
1	–	–	–	–	–	–	–	–	–	–	0
2	–	–	–	–	–	–	–	–	–	–	0
3	–	–	–	–	–	–	1	2	–	–	2
4	–	–	–	–	–	–	–	–	–	–	0
5	–	–	1	2	–	–	–	–	–	–	2
6	–	–	–	–	–	–	–	–	–	–	0
7	–	–	–	–	–	–	–	–	–	–	0
8	–	–	–	1	–	–	–	–	–	–	1
9	–	–	–	–	–	–	–	–	–	–	0
10	–	–	–	–	–	–	–	–	–	–	0
11	–	–	–	–	–	–	1	2	3	4	4
12	–	–	1	2	–	–	–	–	–	3	3
13	1	2	–	–	–	–	–	–	3	4	4
14	1	2	3	4	–	–	–	–	5	6	6
15	–	–	–	–	–	1	2	3	–	–	3
16	1	2	–	–	–	–	–	–	–	–	2
17	–	1	–	–	–	–	–	–	–	–	1
18	1	2	–	–	–	–	3	4	–	–	4
19	–	–	1	–	–	–	2	3	–	–	3
20	–	–	1	–	2	3	4	5	6	7	7

tractably computed by adopting the powerful Stein-Chen method. And some numerical experiments are carried out to investigate the performance of the Stein-Chen approximation method. Furthermore, a comparison of the proposed chart with np_x chart shows that the proposed chart outperforms np_x chart in detecting the same autocorrelated processes. Interestingly, the corresponding in-control average run length (ARL_0) of the proposed chart closes to the allowed minimum value while the out-of-control average run length (ARL_1) is relatively small. In contrast, np_x chart cannot trade off the ARL_0 and ARL_1 well which results in a too large ARL_1 or a too small ARL_0. Next, we conduct a comparison between the proposed chart and np_x chart when autocorrelated data doesn't conform $AR(1)$ process, it turns out that the performance of the proposed chart is better than the np_x chart. Moreover, a sensitivity analysis gives some suggestions for better implementation of the proposed chart. Finally, an industry example for a yogurt cup filling process is utilized to illustrate the use of the proposed chart. The results showed that the proposed chart may use a larger sample size and/or sampling frequency based on equal inspection cost, and therefore has a higher or substantially higher detection effectiveness than the chart proposed by Costa and Castagliola (2011).

In summary, we address the following management insights for implementing the proposed chart: (1) The Stein-Chen approximation method for calculating the average run length (ARL) performs better as the sample size n increases; (2) the proposed chart performs better when the observations of the quality characteristic are highly negative correlation or lowly positive correlation; (3) If autocorrelated process deviates from an $AR(1)$ model, it has an effect on the performance of the proposed chart. Although this effect is relatively small when the correlation is small, it is suggested that it is better to estimate whether the structure of the data fits $AR(1)$ model before using the proposed chart.

The proposed chart is applicable in a mass production environment where the process variables are highly autocorrelated and the attribute inspection is simple to accomplish. However, it may not be suitable to a high-quality environment in which the mean shift of the quality characteristics and the defective rate are extremely small. Many scholars identified that cumulative count of conforming (CCC) control charts are effective in high-quality production environments like Zhang, Xie, and

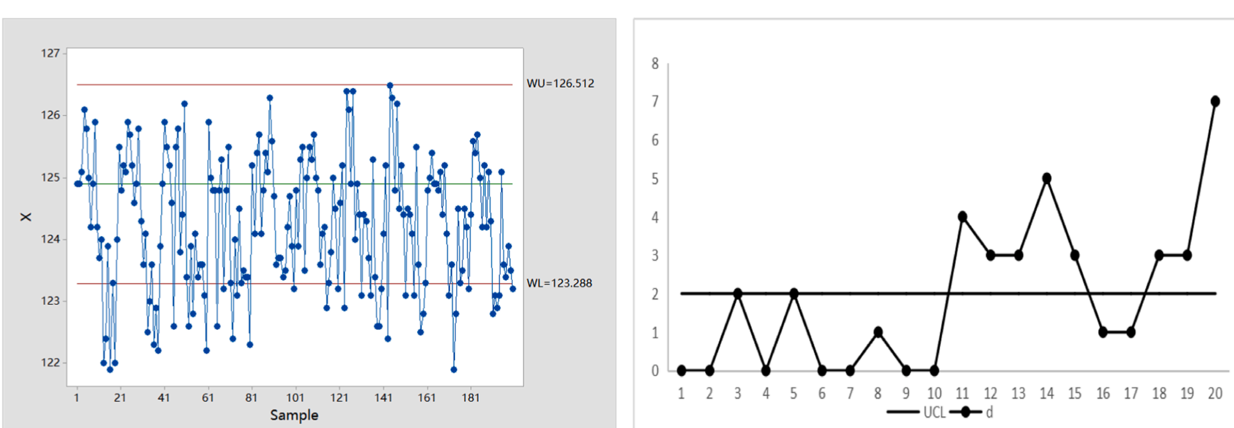

(b_1) The scatter plot of attribute inspection (b_2) The scatter plot of $AR - np_x$ chart

Fig. 7. $AR - np_x$ chart for monitor the mean shifts of yogurt cup weights.

Jin (2012). Moreover, Xie, Goh, and Kuralmani (2012) also presented lots of techniques of implementing control charts for high-quality processes. In future work, it is potential to combine those techniques with the $AR - np_x$ chart to monitor high-quality processes. In addition, the design of the proposed chart is based on $AR(1)$ process. As the numerical experiments showed that the proposed charts may not perform well when autocorrelated process deviates from an $AR(1)$ model, it is also worth considering other autocorrelated data structure in future work.

Acknowledgements

This research is supported by the National Natural Science Foundation of China (NSFC: 71731006, 71571070, 71790615, 71431006 and 71801096), the Project funded by China Postdoctoral Science Foundation under 2019M650202, the Project supported by GDHVPS (2017), the Natural Science Foundation of Guangdong Province under 2015A030311032, and the Fundamental Research Funds for the Central Universities, SCUT (X2gs/D2191820).

Appendix A

Data set which consists of 200 observations of the weight of yogurt cup in industry example is shown in Table 11.

Table 11
The data set of the weight of yogurt cup.

Sample number	X_1	X_2	X_3	X_4	X_5	X_6	X_7	X_8	X_9	X_{10}
1	124.9	124.8	125.9	125.9	125.2	124.8	124.6	124.1	124.8	124.4
2	124.9	125.2	125.5	125.0	124.1	123.9	125.2	125.2	125.0	125.6
3	125.1	125.1	125.2	124.8	125.4	125.3	122.9	122.4	125.4	125.4
4	126.1	125.9	124.6	124.8	125.7	125.5	126.4	126.5	124.9	125.7
5	125.8	125.7	122.6	122.6	124.1	123.5	126.1	126.3	124.9	125.0
6	125.0	125.2	125.5	124.8	124.8	125.0	124.9	124.8	124.8	124.2
7	124.2	124.6	125.8	125.3	125.4	125.5	126.4	126.2	125.1	125.2
8	124.9	124.9	123.8	123.2	125.1	125.3	124.0	124.5	124.4	124.2
9	125.9	125.8	124.4	124.8	126.3	125.7	124.9	125.2	125.2	125.1
10	124.2	124.3	126.2	125.5	125.6	125.0	124.4	124.4	124.1	124.3
11	123.7	123.6	123.4	123.3	124.7	124.8	123.1	123.1	123.1	122.8
12	124.0	124.1	122.6	122.4	123.6	123.6	124.4	124.5	123.6	123.1
13	122.0	122.5	123.9	124.0	123.7	124.1	124.3	124.4	121.9	122.9
14	122.4	123.0	122.8	123.1	123.7	124.2	123.7	124.1	122.8	123.1
15	123.9	123.6	124.1	124.5	123.4	122.9	123.1	123.1	124.5	125.1
16	121.9	122.3	123.4	123.3	123.5	123.3	125.3	125.5	123.3	123.6
17	123.3	122.9	123.6	123.5	124.2	123.8	123.4	123.6	123.5	123.4
18	122.0	122.2	123.6	123.4	124.7	125.0	122.6	122.5	124.5	123.9
19	124.0	123.9	123.1	123.4	123.9	124.5	122.6	122.8	124.2	123.5
20	125.5	124.9	122.2	122.3	123.2	123.2	123.2	123.3	123.2	123.2

Appendix B

The proof of Theorem 1. When $i = 1$, the probability that the observation of X_1 in a sample is larger than W_U in state j denoted by $\widehat{p}_1^{\,j}$ and the probability that the observation of X_i in a sample is smaller than W_L in state j denoted by $\widetilde{p}_1^{\,j}$ can be easily obtained as follows:

$$\widehat{p}_1^{\,j} = P\left\{X_1 > W_U\right\} = P\left\{\frac{X_1 - \mu_j}{\sigma_0} \geqslant \frac{W_U - \mu_j}{\sigma_0}\right\} = 1 - \phi\left(\frac{W_U - \mu_j}{\sigma_0}\right),$$

$$\widetilde{p}_1^{\,j} = P\left\{X_1 < W_L\right\} = P\left\{\frac{X_1 - \mu_j}{\sigma_0} < \frac{W_L - \mu_j}{\sigma_0}\right\} = \phi\left(\frac{W_L - \mu_j}{\sigma_0}\right),$$

Then nonconformities rate of the observation of X_1 is calculated as

$$p_1^{\,j} = P\left\{X_1 > W_U\right\} + P\left\{X_1 < W_L\right\} = 1 - \phi\left(\frac{W_U - \mu_j}{\sigma_0}\right) + \phi\left(\frac{W_L - \mu_j}{\sigma_0}\right).$$

Due to the autocorrelation property shown in Eq. (20), all the probabilities $\widehat{p}_2^{\,j}$, $\widetilde{p}_2^{\,j}$ and $p_2^{\,j}$ depend on $\widehat{p}_1^{\,j}$, $\widetilde{p}_1^{\,j}$ and $p_1^{\,j}$. Based on the Law of Total Probability, we have

$$\begin{aligned}
\widehat{p}_2^{\,j} &= P\{X_2 > W_U\} \\
&= P\{X_2 > W_U | X_1 > W_U\}P\{X_1 > W_U\} + P\{X_2 > W_U | X_1 < W_L\}P\{X_1 < W_L\} \\
&\quad + P\{X_2 > W_U | W_L \leqslant X_1 \leqslant W_U\}P\{W_L \leqslant X_1 \leqslant W_U\} \\
&= \widehat{p}_1^{\,j}\int_{W_U}^{+\infty} P\left\{\rho\left(X_1 - \mu_j\right) + \varepsilon_1 + \mu_j > W_U\right\} f(X_1)dX_1 \\
&\quad + \widetilde{p}_1^{\,j}\int_{-\infty}^{W_L} P\{\rho(X_1 - \mu_j) + \varepsilon_1 + \mu_j > W_U\} f(X_1)dX_1 \\
&\quad + \left(1 - \widehat{p}_1^{\,j} - \widetilde{p}_1^{\,j}\right)\int_{W_L}^{W_U} P\left\{\rho\left(X_1 - \mu_j\right) + \varepsilon_1 + \mu_j > W_U\right\} f(X_1)dX_1 \\
&= \widehat{p}_1^{\,j}\int_{W_U}^{+\infty} P\left\{\frac{\varepsilon_1 - 0}{\sqrt{1-\rho^2}\sigma_0)} > \frac{W_U - \rho\left(X_1 - \mu_j\right) - \mu_j}{\sqrt{1-\rho^2}\sigma_0)}\right\} f(X_1)dX_1 \\
&\quad + \widetilde{p}_1^{\,j}\int_{-\infty}^{W_L} P\left\{\frac{\varepsilon_1 - 0}{\sqrt{1-\rho^2}\sigma_0)} > \frac{W_U - \rho\left(X_1 - \mu_j\right) - \mu_j}{\sqrt{1-\rho^2}\sigma_0)}\right\} f(X_1)dX_1 \\
&\quad + \left(1 - \widehat{p}_1^{\,j} - \widetilde{p}_1^{\,j}\right)\int_{W_L}^{W_U} P\left\{\frac{\varepsilon_1 - 0}{\sqrt{1-\rho^2}\sigma_0)} > \frac{W_U - \rho\left(X_1 - \mu_j\right) - \mu_j}{\sqrt{1-\rho^2}\sigma_0)}\right\} f(X_1)dX_1 \\
&= \widehat{p}_1^{\,j}\int_{W_U}^{+\infty}\left(1 - \phi\left(\left(W_U - \rho\left(X_1 - \mu_j\right) - \mu_j\right)/\sqrt{1-\rho^2}\sigma_0\right)\right) f(X_1)dX_1 \\
&\quad + \widetilde{p}_1^{\,j}\int_{-\infty}^{W_L}(1 - \phi((W_U - \rho(X_1 - \mu_j) - \mu_j)/\sqrt{1-\rho^2}\sigma_0)) f(X_1)dX_1 \\
&\quad + \left(1 - \widehat{p}_1^{\,j} - \widetilde{p}_1^{\,j}\right)\int_{W_L}^{W_U}\left(1 - \phi\left(\left(W_U - \rho\left(X_1 - \mu_j\right) - \mu_j\right)/\sqrt{1-\rho^2}\sigma_0\right)\right) f(X_1)dX_1
\end{aligned} \tag{21}$$

and

$$\begin{aligned}
\widetilde{p}_2^{\,j} &= P\{X_2 < W_L\} \\
&= P\{X_2 < W_L | X_1 > W_U\}P\{X_1 > W_U\} + P\{X_2 < W_L | X_1 < W_L\}P\{X_1 < W_L\} \\
&\quad + P\{X_2 < W_L | W_L \leqslant X_1 \leqslant W_U\}P\{W_L \leqslant X_1 \leqslant W_U\} \\
&= \widehat{p}_1^{\,j}\int_{W_U}^{+\infty} P\left\{\rho\left(X_1 - \mu_j\right) + \varepsilon_1 + \mu_j < W_L\right\} f(X_1)dX_1 \\
&\quad + \widetilde{p}_1^{\,j}\int_{-\infty}^{W_L} P\{\rho(X_1 - \mu_j) + \varepsilon_1 + \mu_j < W_L\} f(X_1)dX_1 \\
&\quad + \left(1 - \widehat{p}_1^{\,j} - \widetilde{p}_1^{\,j}\right)\int_{W_L}^{W_U} P\left\{\rho\left(X_1 - \mu_j\right) + \varepsilon_1 + \mu_j < W_L\right\} f(X_1)dX_1 \\
&= \widehat{p}_1^{\,j}\int_{W_U}^{+\infty} P\left\{\frac{\varepsilon_1 - 0}{\sqrt{1-\rho^2}\sigma_0)} < \frac{W_L - \rho\left(X_1 - \mu_j\right) - \mu_j}{\sqrt{1-\rho^2}\sigma_0)}\right\} f(X_1)dX_1 \\
&\quad + \widetilde{p}_1^{\,j}\int_{-\infty}^{W_L} P\left\{\frac{\varepsilon_1 - 0}{\sqrt{1-\rho^2}\sigma_0)} < \frac{W_L - \rho\left(X_1 - \mu_j\right) - \mu_j}{\sqrt{1-\rho^2}\sigma_0)}\right\} f(X_1)dX_1 \\
&\quad + \left(1 - \widehat{p}_1^{\,j} - \widetilde{p}_1^{\,j}\right)\int_{W_L}^{W_U} P\left\{\frac{\varepsilon_1 - 0}{\sqrt{1-\rho^2}\sigma_0)} < \frac{W_L - \rho\left(X_1 - \mu_j\right) - \mu_j}{\sqrt{1-\rho^2}\sigma_0)}\right\} f(X_1)dX_1 \\
&= \widehat{p}_1^{\,j}\int_{W_U}^{+\infty}\phi\left(\left(W_L - \rho\left(X_1 - \mu_j\right) - \mu_j\right)/\sqrt{1-\rho^2}\sigma_0\right) f(X_1)dX_1 \\
&\quad + \widetilde{p}_1^{\,j}\int_{-\infty}^{W_L}\phi((W_L - \rho(X_1 - \mu_j) - \mu_j)/\sqrt{1-\rho^2}\sigma_0) f(X_1)dX_1 \\
&\quad + \left(1 - \widehat{p}_1^{\,j} - \widetilde{p}_1^{\,j}\right)\int_{W_L}^{W_U}\phi\left(\left(W_L - \rho\left(X_1 - \mu_j\right) - \mu_j\right)/\sqrt{1-\rho^2}\sigma_0\right) f(X_1)dX_1.
\end{aligned} \tag{22}$$

Then, nonconformities rate of the observation of X_2 is calculated as

$$
\begin{aligned}
p_2^j = &\ \widehat{p}_2^{\,j} + \widetilde{p}_2^{\,j} \\
&= \widehat{p}_1^{\,j} \int_{W_U}^{+\infty} \left(1 - \phi\left(\left(W_U - \rho\left(X_1 - \mu_j\right) - \mu_j\right)/\sqrt{1-\rho^2}\sigma_0\right)\right) \\
&+ \phi((W_L - \rho(X_1 - \mu_j) - \mu_j)/\sqrt{1-\rho^2}\sigma_0))f(X_1)dX_1 \\
&+ \widetilde{p}_1^{\,j} \int_{-\infty}^{W_L} ((1 - \phi((W_U - \rho(X_1 - \mu_j) - \mu_j)/\sqrt{1-\rho^2}\sigma_0))) \\
&+ \phi((W_L - \rho(X_1 - \mu_j) - \mu_j)/\sqrt{1-\rho^2}\sigma_0))f(X_1)dX_1 \\
&+ \left(1 - \widehat{p}_1^{\,j} - \widetilde{p}_1^{\,j}\right) \int_{W_L}^{W_U} \left(\left(1 - \phi\left(\left(W_U - \rho\left(X_1 - \mu_j\right) - \mu_j\right)/\sqrt{1-\rho^2}\sigma_0\right)\right)\right. \\
&+ \phi((W_L - \rho(X_1 - \mu_j) - \mu_j)/\sqrt{1-\rho^2}\sigma_0))f(X_1)dX_1.
\end{aligned} \tag{23}
$$

Based on Eqs. (21)–(23), we can further calculate the probabilities $\widehat{p}_3^{\,j}$, $\widetilde{p}_3^{\,j}$ and p_3^j which have a similar form. Then, summarizing the recurrence relation, we can obtain:

$$
\begin{aligned}
\widehat{p}_i^{\,j} &= \widehat{p}_{i-1}^{\,j} \int_{W_U}^{+\infty} \left(1 - \phi\left(\left(W_U - \rho\left(X_{i-1} - \mu_j\right) - \mu_j\right)/\sqrt{1-\rho^2}\sigma_0\right)\right) f(X_{i-1})dX_{i-1} \\
&= \widetilde{p}_{i-1}^{\,j} \int_{-\infty}^{W_L} (1 - \phi((W_U - \rho(X_{i-1} - \mu_j) - \mu_j)/\sqrt{1-\rho^2}\sigma_0)) f(X_{i-1})dX_{i-1} \\
&= \left(1 - \widehat{p}_{i-1}^{\,j} - \widetilde{p}_{i-1}^{\,j}\right) \int_{W_L}^{W_U} \left(1 - \phi\left(\left(W_U - \rho\left(X_{i-1} - \mu_j\right) - \mu_j\right)/\sqrt{1-\rho^2}\sigma_0\right)\right) f(X_{i-1})dX_{i-1}
\end{aligned}
$$

and

$$
\begin{aligned}
\widetilde{p}_i^{\,j} &= \widehat{p}_{i-1}^{\,j} \int_{W_U}^{+\infty} \phi\left(\left(W_L - \rho\left(X_{i-1} - \mu_j\right) - \mu_j\right)/\sqrt{1-\rho^2}\sigma_0\right) f(X_{i-1})dX_{i-1} \\
&= \widetilde{p}_{i-1}^{\,j} \int_{-\infty}^{W_L} \phi((W_L - \rho(X_{i-1} - \mu_j) - \mu_j)/\sqrt{1-\rho^2}\sigma_0) f(X_{i-1})dX_{i-1} \\
&= \left(1 - \widehat{p}_{i-1}^{\,j} - \widetilde{p}_{i-1}^{\,j}\right) \int_{W_L}^{W_U} \phi\left(\left(W_L - \rho\left(X_{i-1} - \mu_j\right) - \mu_j\right)/\sqrt{1-\rho^2}\sigma_0\right) f(X_{i-1})dX_{i-1}.
\end{aligned}
$$

Then, $p_i^j = \widehat{p}_i^{\,j} + \widetilde{p}_i^{\,j}$ and the Eqs. (4) and (5) are obtained.

Appendix C. Supplementary material

Supplementary data associated with this article can be found, in the online version, at https://doi.org/10.1016/j.cie.2019.106081.

References

Alwan, L. C., & Roberts, H. V. (1988). Time-series modeling for statistical process control. *Journal of Business & Economic Statistics, 6*(1), 87–95.

Arratia, R., Goldstein, L., & Gordon, L. (1990). Poisson approximation and the Chen-Stein method. *Statistical Science, 5*(4), 403–424.

Chen, L. H. Y. (1975). Poisson approximation for dependent trials. *The Annals of Probability,* 534–545.

Chen, A., & Chen, Y. K. (2007). Design of ewma and cusum control charts subject to random shift sizes and quality impacts. *IIE Transactions, 39*(12), 1127–1141.

Chen, H., & Cheng, Y. (2009). Designing $\overline{X}$ charts for known autocorrelations and unknown marginal distribution. *European Journal of Operational Research, 198*(2), 520–529.

Costa, A. F., Branco, M. A., & Machado, G. (2011). Variable parameter and double sampling x charts in the presence of correlation: The markov chain approach. *International Journal of Production Economics, 130*(2), 224–229.

Costa, A. F. B., & Castagliola, P. (2011). Effect of measurement error and autocorrelation on the $\overline{X}$ chart. *Journal of Applied Statistics, 38*(4), 661–673.

Costa, A., & Fichera, S. (2017). Economic statistical design of arma control chart through a modified fitness-based self-adaptive differential evolution. *Computers & Industrial Engineering, 105*, 174–189.

De Ketelaere, B., Rato, T., Schmitt, E., & Hubert, M. (2016). Statistical process monitoring of time-dependent data. *Quality Engineering, 28*(1), 127–142.

Du, S., & Lv, J. (2013). Minimal euclidean distance chart based on support vector regression for monitoring mean shifts of auto-correlated processes. *International Journal of Production Economics, 141*(1), 377–387.

Franco, B. C., Celano, G., Castagliola, P., & Costa, A. F. B. (2014). Economic design of Shewhart control charts for monitoring autocorrelated data with skip sampling strategies. *International Journal of Production Economics, 151*(151), 121–130.

Franco, B. C., Costa, A. F. B., & Machado, M. A. G. (2012). Economic-statistical design of the chart used to control a wandering process mean using genetic algorithm. *Expert Systems with Applications, 39*(17), 12961–12967.

He, Z., Wang, Z., Tsung, F., & Shang, Y. (2016). A control scheme for autocorrelated bivariate binomial data. *Computers & Industrial Engineering, 98*, 350–359.

Ho, L. L., & Quinino, R. C. (2013). An attribute control chart for monitoring the variability of a process. *International Journal of Production Economics, 145*(1), 263–267.

Leoni, R. C., & Costa, A. F. B. (2015). The effect of the autocorrelation on the performance of the t 2 chart. *European Journal of Operational Research, 247*(1), 155–165.

Leoni, R. C., Costa, A. F. B., & Machado, M. A. G. (2015). The effect of the autocorrelation on the performance of the t 2 chart. *European Journal of Operational Research, 247*(1), 155–165.

Li, C., Mukherjee, A., Su, Q., & Xie, M. (2016). Optimal design of a distribution-free quality control scheme for cost-efficient monitoring of unknown location. *International Journal of Production Research, 54*(24), 7259–7273.

Montgomery, D. C. (2007). *Introduction to statistical quality control.* John Wiley & Sons.

Nezhad, M. S., Fallah, S. T., & Niaki, A. (2010). A new monitoring design for uni-variate statistical quality control charts. *Information Sciences, 180*(6), 1051–1059.

Sampaio, E. S., Ho, L. L., & de Medeiros, P. G. (2014). A combined control chart to monitor the process mean in a two-stage sampling. *Quality and Reliability Engineering International, 30*(7), 1003–1013.

Simes, F. D., Leoni, R. C., & Costa, A. F. B. (2016). Synthetic charts to control bivariate processes with autocorrelated data. *Computers & Industrial Engineering, 97*, 15–25.

Singh, S. (2013). Robustness to non-normality and ar (2) process of control charts. *International Journal of Scientific and Research Publications, 3*(11), 1–10.

Stein, C. (1972). A bound for the error in the normal approximation to the distribution of a sum of dependent random variables. *Proceedings of the Sixth Berkeley Symposium on Mathematical Statistics and Probability: Probability Theory: vol. 2*The Regents of the University of California.

Vanhatalo, E., & Kulahci, M. (2015). The effect of autocorrelation on the hotelling t^2 control chart. *Quality and Reliability Engineering International, 31*(8), 1779–1796.

Wardell, D. G., Moskowitz, H., & Plante, R. D. (1994). Run-length distributions of specialcause control charts for correlated processes. *Technometrics, 36*(1), 3–17.

Wu, Z., & Jiao, J. (2008). A control chart for monitoring process mean based on attribute inspection. *International Journal of Production Research, 46*(15), 4331–4347.

Wu, Z., Khoo, M. B. C., Shu, L., & Jiang, W. (2009). An np control chart for monitoring the mean of a variable based on an attribute inspection. *International Journal of Production Economics, 121*(1), 141–147.

Xie, M., Goh, T. N., & Kuralmani, V. (2012). *Statistical models and control charts for high-quality processes.* Springer Science & Business Media.

Xu, X. H., & Huang, A. (2014). Model-based multivariate monitoring charts for auto-correlated processes. *Quality and Reliability Engineering International, 30*(4), 527–543.

Zhang, C. W., Xie, M., & Jin, T. (2012). An improved self-starting cumulative count of conforming chart for monitoring high-quality processes under group inspection. *International Journal of Production Research, 50*(23), 7026–7043.